X-625-70-394
PREPRINT

NASA TM X-65369

THE BEHAVIOR OF THE IONOSPHERE ABOVE WALLOPS ISLAND DURING THE ECLIPSE OF 7 MARCH 1970

J. E. JACKSON
C. J. McQUILLAN

OCTOBER 1970

GODDARD SPACE FLIGHT CENTER
GREENBELT, MARYLAND

THE BEHAVIOR OF THE IONOSPHERE ABOVE WALLOPS ISLAND DURING THE ECLIPSE OF 7 MARCH 1970

by

J. E. Jackson
C. J. McQuillan
Laboratory for Planetary Atmospheres
NASA/Goddard Space Flight Center
Greenbelt, Maryland

ABSTRACT

The variation of the ionospheric electron density above Wallops Island during the solar eclipse of 7 March 1970 was investigated using ionograms obtained from 1200 to 1600 EST on March 7 and on March 6 (control day). Comparison of the normalized densities (March 7 values/March 6 values) at fixed heights to the obscuration function indicates that 7 percent of the total ionizing flux was of coronal origin and that more flux originated from the Eastern half of the sun than from the Western half. The results are consistent with the East-West solar scans of the Algonquin Radio Observatory. The normalized densities were also compared to the theoretical prediction made by Stubbe prior to the eclipse. The difference between prediction and observation is due partly to the uniform disk radiation assumed by Stubbe.

INTRODUCTION

A solar eclipse provides a unique opportunity for the investigation of a number of ionospheric problems. One group of problems is broadly concerned with studies of the ionizing sources which can be deduced from correlations between the solar obscuration and the resulting ionization. Another group of studies is concerned with the various production and loss mechanisms which control the response of the ionosphere at various altitudes. Eclipse effects on the ionosphere were first inferred from observations made during the eclipse of 17 April 1912. Since then, the ionospheric effects of about 40 solar eclipses have been studied with increasingly refined and comprehensive techniques.

The eclipse of 7 March 1970 was of special interest for a number of reasons. It offered a long period of totality (ranging from 2 to 3 minutes), and was visible at midday (when the solar zenith angle is relatively constant) from very accessible regions of the earth. In addition, the path of totality came very close to the rocket launch sites at Elgin Gulf Test Range, Florida (1) and Wallops Island, Virginia (2). A temporary launch site was also set up near East Quoddy, Nova Scotia (3). The above circumstances made it possible to conduct very comprehensive observations, including in situ measurements of many ionospheric parameters, such as the density, composition, and temperature of both the neutral and ionized constituents. The unusual opportunity for correlative

studies makes it particularly desirable to analyze in detail the ionosonde observations at Wallops Island.

EXPERIMENTAL DATA

For the geographical coordinates of the Wallops Island ionosonde (37.88^{o} N, 75.48^{o}W) the maximum obscuration (4) was 98.99% at 150 km (1340:09 EST) and 98.02% at 250 km (1341:42 EST). Since the ionospheric response follows most closely the obscuration function at altitudes of 150 km or less, the obscuration function (4) for 150 km was used for the present study. At this altitude the eclipse began at 1223 EST and ended at 1454 EST. During the eclipse, the solar zenith angle at Wallops Island varied from 43.1^{o} at first contact, to 47.5^{o} at totality, to 57.0^{o} at last contact; the sunspot number was 108 (the previous 27 day mean was 133.7); the 2800 MHz solar flux (Ottawa) adjusted to 1 a.u. was 168.4 (the previous 27 day mean was 181.8); the magnetic index AP was 42 (it rose to 149 on the following day). The days prior to the eclipse were fortunately relatively quiet and the data for March 6 (Ap = 25) were used as reference levels. A solar flare (rated between class 1 and 2) was in progress about one hour prior to the beginning of the eclipse at Wallops Island. This flare began at 1100 EST and lasted until 1150 EST. There were also two subflares close to the time of the eclipse, one starting at 1023 EST and the other one starting at 1517 EST. The J-5 ionosonde in use at Wallops Island provides soundings from 200 kHz to 20 MHz. Ionograms were taken at 30 second intervals during most of the eclipse. The high quality of

these ionograms is indicated by the examples shown on Fig. 1 for the first half of the eclipse and on Fig. 2 for the second half of the eclipse. The ionograms for March 6, 1970 are not shown but they are similar to the March 7 ionogram at 1259 EST.

QUALITATIVE OBSERVATIONS

The ionograms were much more disturbed during the second half of the eclipse (see ionograms for 1340, 1347 and 1424) than during the first half of the eclipse (see ionograms for 1259 and 1320). The 1259 and 1424 ionograms correspond to the same solar obscuration (about 35% of the solar disk covered), yet the 1424 ionogram exhibits much more spread in the E-region and more intense sporadic E echoes. Prior to the eclipse the ionograms were similar to that of 1259. The sporadic E echoes increased slightly in intensity during the first half of the eclipse, and became much more intense during the second half. The sporadic E became weaker at the end of the eclipse, but it was still moderately strong 20 minutes later (see 1519 ionogram). Oblique echoes became quite pronounced at maximum phase (1340 ionogram) and during the second half of the eclipse. There was no evidence of an F1.5 cusp, which is consistent with previous midlatitude eclipse observations (5). Also typical is the enhancement of the F1 cusp near totality and during the second half of the eclipse (5). It is also of interest to note the appearance of echoes at the low frequency end of the ionogram at totality and during the second part of the eclipse.

On the control day during the corresponding period of time the ionograms showed either weak or no sporadic E. There was no spread, no oblique echoes, no echoes below 1.5 MHz, and very weak F1 cusps.

ELECTRON DENSITY PROFILES

A selection of ionograms taken between noon and 4 pm on the eclipse day and on the previous day were used to calculate the corresponding electron density profiles. The techniques used to analyze the ionograms are discussed in the Appendix. Typical profiles corresponding to the first part of the eclipse are shown in Fig. 3. It is seen that the decay is monotonic at all altitudes and quite uniform below 200 km. The valley above Emax is shown as a dashed line because some assumptions are required in the valley calculation (see Appendix). Typical profiles for the recovery phase are shown in Fig. 4. The recovery is fairly uniform up to altitudes of about 180 km, but at higher altitudes the densities continue to decay past the time of maximum obscuration. This time delay is more clearly shown in Fig. 5 where densities at constant heights are plotted as a function of time. The minimum for each of the curves of Fig. 5 coincides very closely with maximum obscuration up to 180 km but occurs at increasingly later times at altitudes above 180 km. The profiles of Fig. 5 also exhibit a depression just prior to the beginning of the eclipse. This disturbance is probably related to the solar flare which occurred one hour prior to the beginning of the eclipse. The ionospheric behavior for the corresponding time period on the

previous day is shown in Fig. 6. The densities at constant heights on March 6 were quite uniform. The 150 km contour may appear somewhat irregular but this may be due largely to the uncertainty arising from the E-valley calculation. This uncertainty affects mostly the region immediately above the valley; it has little effect upon the contours above 150 km (see Appendix).

DISCUSSION OF RESULTS

In a recent paper (6) Stubbe predicted the behavior of the ionosphere above Wallops Island during the 7 March 1970 eclipse and calculated the expected density variation at 150, 180, 210, 240, 270 and 300 km. To permit a comparison with Stubbe's predictions the results of the present ionogram analysis have been given for these altitudes (except at 300 km since in many cases this altitude was beyond the range of the ionogram data). Simplified theoretical considerations also predict that the electron density variation in the lower portion of the ionosphere should be proportional to the square root of the incident ionizing flux, i.e. to the square root of the obscuration function for a uniform disk. The experimental results, Stubbe's predictions and the $[\text{obscuration}]^{1/2}$ curve are compared in Figures 7 and 8. The experimental curves were normalized by taking the ratio of the eclipse day to the control day densities. Stubbe's curves were normalized in the same manner. At Emax, 150 km and 180 km (Fig. 7) the minimum of the normalized experimental data is in phase with

but greater than the minimum of the [obscuration]$^{1/2}$ curve. The value of this minimum is also remarkably consistent on the 3 curves. Stubbe did not show an Emax curve, but the minimum for Stubbe's curves at 150 and at 180 km is closer in value to the [obscuration]$^{1/2}$ curve. Stubbe's curves for these altitudes also exhibit a small time delay which is not seen on the experimental data. The experimental curves for 210, 240 and 270 km (Fig. 8) reveal a time delay for the minimum which is comparable to the delay predicted by Stubbe at 210 km, but greater than predicted at 240 and 270 km.

The difference between the experimental data and the [obscuration]$^{1/2}$ curve is attributed to flux from the unobscured corona and to non-uniformity of the radiation from the solar disk. The [obscuration]$^{1/2}$ curve was recomputed by assuming that a fixed percentage of the ionizing flux came from the corona and was not subject to obscuration. The percentage was determined by assuming that the minimum value of the [obscuration]$^{1/2}$ curve should agree with the minimum value of curve 2 at Emax (Figure 7). The resulting coronal flux was 7 percent of the total flux. This is consistent with the results of similar calculations performed for other solar eclipses, which show typically that 10 to 20 percent of the ionizing flux is of coronal origin. This modified [obscuration]$^{1/2}$ curve is a first order estimate of the variation in electron density which one might expect at Emax, and the difference between the two is a measure of the non-uniformity of the solar disk radiation.

This difference is the quantity $\Delta\phi$ shown as a function of time on Figure 9. Also shown on Figure 9 is the visible obscuration of the disk at various times. These times are also indicated by arrows next to the $\Delta\phi$ curve. It is seen that $\Delta\phi$ is positive at 1300 and 1320, i.e. greater than expected from a uniform disk. It is also seen that at those two times the very active regions (617 and 618) on the eastern side of the sun are still uncovered, which suggests that these regions are responsible for the flux excess on the eastern half of the sun. Conversely at 1400, 1420 and 1430 when these regions are covered there is a deficiency of flux. The correlation is poorer at 1440 where regions 617 and 618 appear fairly well uncovered and $\Delta\phi$ is still negative. The overall picture, nevertheless, leads one to conclude that more ionizing flux originated from the eastern side of the sun than from the western side. This is consistent with the 10.7 cm East-West solar scan conducted by the Algonquin Radio Observatory, Canada at 1723 UT on 7 March 1970, which shows that 65% of the total 10.7 cm flux came from the eastern half of the sun. The East-West scans also show that 8 percent of this flux came from outside of the photosphere. The East-West asymmetry and the coronal flux are certainly factors which contribute to the difference between Stubbe's predictions and the experimental observations. A more complete evaluation of Stubbe's analysis cannot be made until his calculations are repeated using a more realistic variation of the ionizing flux.

APPENDIX

Calculation of Electron Density Profiles from the Ionograms

There are two basic and well-known problems associated with the calculation of electron density profiles from daytime ground-based soundings. First, the ionograms usually exhibit a major discontinuity because the electron density does not increase monotonically with altitude from the E to the F regions (E-valley problem). Second, the ionograms do not show echoes for f<1.0 MHz (starting point problem). Fortunately some experimental data are available which can be used to reduce the above uncertainties, and in some cases the joint use of both ordinary and extraordinary echoes can provide estimates of the depth of the E-valley.

Midday rocket measurements at Wallops Island (7) have shown that the electron density at 80 km is typically 1000 el/cc and that this density increases exponentially up to the density at which the ionosonde data begins. Cross modulation experiments conducted at Kjeller, Norway (8) gave midday electron densities at 80 km ranging from 1000 to 4000 el/cc. In the actual analysis it was assumed that the density at 80 km was a fixed percentage (2%) of the density at Emax, thereby introducing some correction for the obscuration. Below 80 km the density is assumed to be zero. Changing the assumed density at 80 km by a factor of 2 changes the densities shown at 150, 180, 210, 240 and 270 km by typically less than 2%.

Midlatitude, midday rocket data (9), (10) show that the minimum E-valley density is typically 80 to 90% of the density

at Emax. This result has also been supported by calculations based upon the joint use of the ordinary and extraordinary traces in ionograms (11). The "start" and "valley" assumptions are illustrated graphically on Figure 10 which shows the resulting profile (for 1519 EST on 7 March 1970) for no E-valley, an 80% valley and a 60% valley. The shape of the valley (a triangular wedge on this semi-logarithmic plot) is one of many assumed by other authors (11), (12). It is physically unrealistic but convenient for computer programming. Furthermore the shape of the valley is too variable to justify the use of a more aesthetic representation. The purpose of the valley is to modify the profile above the valley (rather than to provide meaningful data within the valley). The profiles shown in Fig. 10 would normally be derived from the ordinary trace. These profiles and two additional ones for a 90% and a 70% valley respectively have been used to compute the family of extraordinary traces above Emax shown in Fig. 11. The solid data which represent the observed X-trace are seen to agree best with a valley of 80%.

Ionograms, unfortunately, do not always lend themselves to the type of verification illustrated in Fig. 11. Had we attempted to do likewise with the ionogram for 1259 EST on 7 March 1970, the result would have been as shown on Fig. 12. In this case the test would be inconclusive because the separation between the computed X-traces is small compared to the scaling uncertainty. With no error in scaling one would expect the measured points to agree with the calculated curves in the

region where these curves converge. Since the computed X-traces are based upon profiles derived from O-traces, the computed X-traces are affected by errors in the O-trace scaling. Thus the discrepancy shown on Fig. 12 arises from errors in the scaling of both the O- and the X-traces.

The ionograms used for the eclipse study were analyzed assuming that the E valley was 80% of Emax in all cases, since this value seemed to be representative for midlatitude, midday conditions, and also since this value gave a satisfactory O-trace, X-trace agreement in the cases when this test could be performed. Based upon available evidence, it seems very unlikely that the valley minimum was less than 70% or greater than 90% of Emax for the profile at 1519 EST on 7 March 1970. This would yield a maximum uncertainty in density of $\pm$ 13% at 150 km, $\pm$ 7% at 210 km and $\pm$ 1% at 270 km. The analysis technique and associated formulas were basically the same as those used for topside ionograms (13). In fact, the program used is a modification of the topside program in which the ground-based sounding (with the virtual heights reduced by 80 km) are treated as ionograms obtained from a sounder located at an altitude of 80 km. In view of the many improvements required and incorporated in programs for the reduction of topside ionograms (13), the retention of these features in the analysis of ground-based soundings makes this analysis slightly more refined than is really necessary.

REFERENCES

(1) Faire, A.C., "Rocket Density Measurements at Eglin, Florida", Nature, Vol. 226, June 20, 1970, p. 1110-1111.

(2) Accardo, C.A., "The March Eclipse Rocket Program at Wallops Island", Sky and Telescope, June 1970, p. 344-349.

(3) Belrose, J.S., McNamara, A.G., Hall, J.E., Bode, L.R., Bunker, R., Ross, D.B., Dickinson, P.H.G. and Hall, A.J., "Changes in the Lower Ionosphere during the Eclipse: A Preliminary Report of the Canadian Programme", Nature, Vol. 226, June 20, 1970, p.1100-1107.

(4) Daly, C.J. (Goddard Space Flight Center), private communication, April 1970.

(5) DeJager, C. and Gledhill, J.A., "The Enhancement of the F1-cusp and the Appearance of the F1½-layer During Solar Eclipses", Journal of Atmospheric and Terrestrial Physics, 1963, Vol. 25, pp. 403-413.

(6) Stubbe, P., "The F-region during an eclipse - A theoretical study", Journal of Atmospheric and Terrestrial Physics, June 1970, Vol. 32, No. 6, p. 1109-1116.

(7) Bourdeau, R.E., Aikin, A.C., and Donley, J.L., "Lower Ionosphere at Solar Minimum", Journal of Geophysical Research, Feb. 1, 1966, Vol. 71, No. 3, p. 727-740.

(8) Barrington, R.E., Thrane, E.V., and Bjelland, B., "Diurnal and Seasonal Variations in D-Region Electron Densities Derived from Observations of Cross Modulation", Canadian Journal of Physics, Feb. 1963, Vol. 41, No. 2, p. 271-285.

(9) Seddon, J.C. and Jackson, J.E., "Ionosphere Electron Densities and Differential Absorption", Annales de Geophysique, Oct.-Dec., 1958, Tome 14, No. 4, p. 456-463.

(10) Bauer, S.J. and Jackson, J.E., "A Small Multi-Purpose Rocket Payload for Ionospheric Studies", Goddard Space Flight Center document X-615-63-95 presented at the Fourth International Space Sciences Symposium (COSPAR) in Warsaw, Poland, June 3-11, 1963.

(11) Davies, K., and Saha, A.K., "Study of the 'Valley Problem' with a Ray Tracing Program", p. 162-166 in Electron Density Profiles in the Ionosphere and Exosphere, edited by B. Maehlum, New York, Pergamon Press, 1962.

(12) Mal'tseva, O.A., "Method of Correcting the N(h) Profiles of the F-region with Allowance for a 'Valley'", Geomagnetism and Aeronomy, 1969, Vol. IX, No. 5, p. 753-755.

(13) Jackson, J.E., "The Reduction of Topside Ionograms to Electron-Density Profiles", Proceedings of the IEEE, June 1969, Vol. 57, No. 6, p. 960-976.

FIGURE CAPTIONS

Figure 1. Representative Wallops Island ionograms taken during the first half of the eclipse.

Figure 2. Representative Wallops Island ionograms taken during the second half of the eclipse.

Figure 3. Representative electron density profiles over Wallops Island during the first half of the eclipse.

Figure 4. Representative electron density profiles over Wallops Island during the second half of the eclipse.

Figure 5. Electron density at fixed altitudes during the eclipse.

Figure 6. Electron density at fixed altitudes for the control day.

Figure 7. Normalized observations and predictions (Stubbe) compared to the square root of the obscuration function.

Figure 8. Normalized observations and predictions (Stubbe) compared to the square root of the obscuration function.

Figure 9. Obscuration of the solar disk and the quantity $\Delta\phi = \phi_1 - \phi_2$, where ϕ_1 is the percent flux inferred from the electron density variation at Emax and ϕ_2 is the percent flux based upon the obscuration of a uniform disk emitting 93% of the total flux.

Figure 10. Diagram illustrating assumptions made in the analysis of ground-based ionospheric soundings.

Figure 11. Calculated X traces for electron density profiles based upon the O-trace analysis and for various assumed E-valley depths.

Figure 12. Calculated X traces for electron density profiles based upon the O-trace analysis and for various assumed E-valley depths.

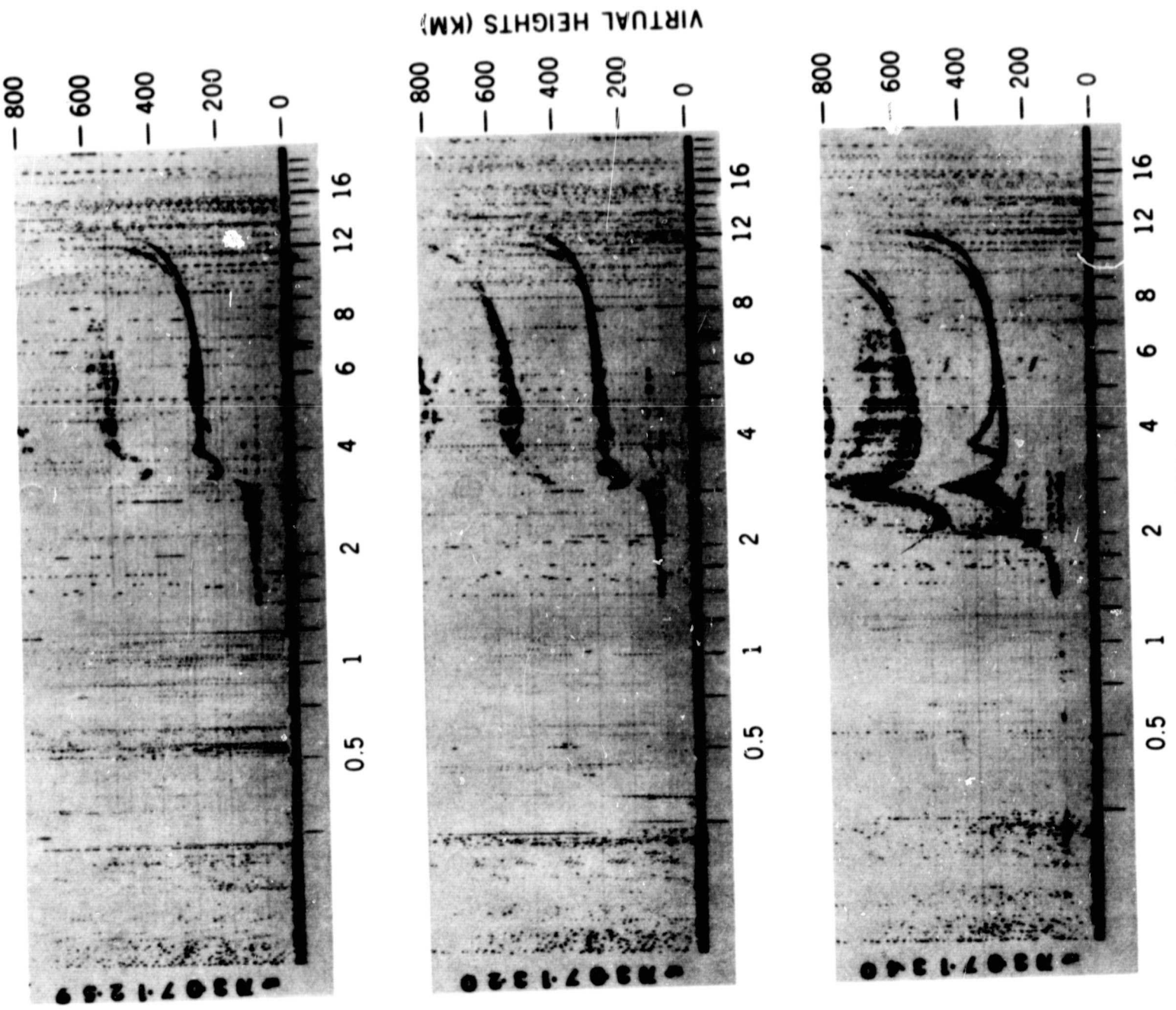
VIRTUAL HEIGHTS (KM)
800
600
400
200
0
0.5
1
2
4
6
8
12
16
FREQUENCY (MHz)

Figure 1

Figure 2

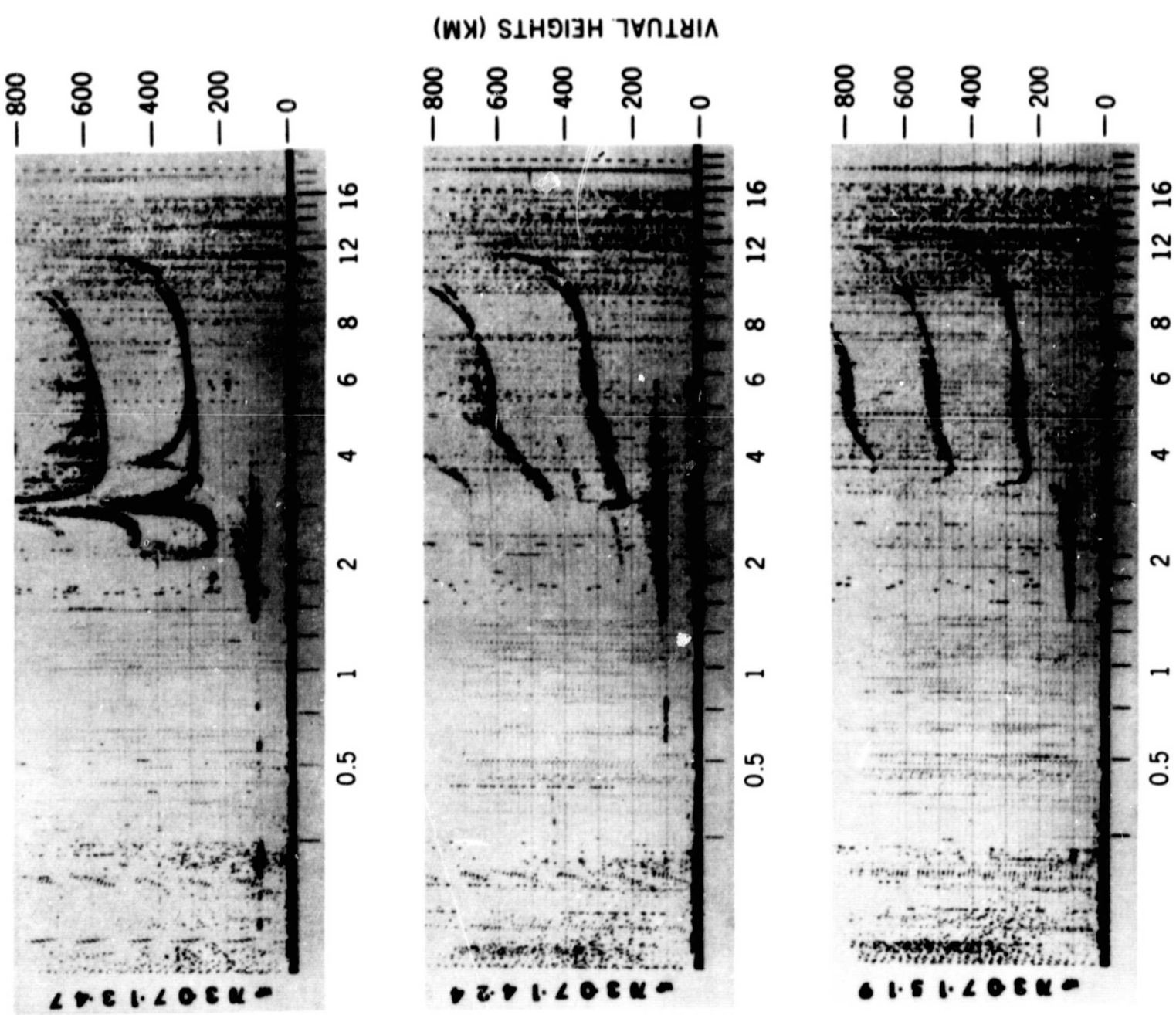
VIRTUAL HEIGHTS (KM)
800
600
400
200
0
0.5
1
2
4
6
8
12
16
FREQUENCY (MHz)

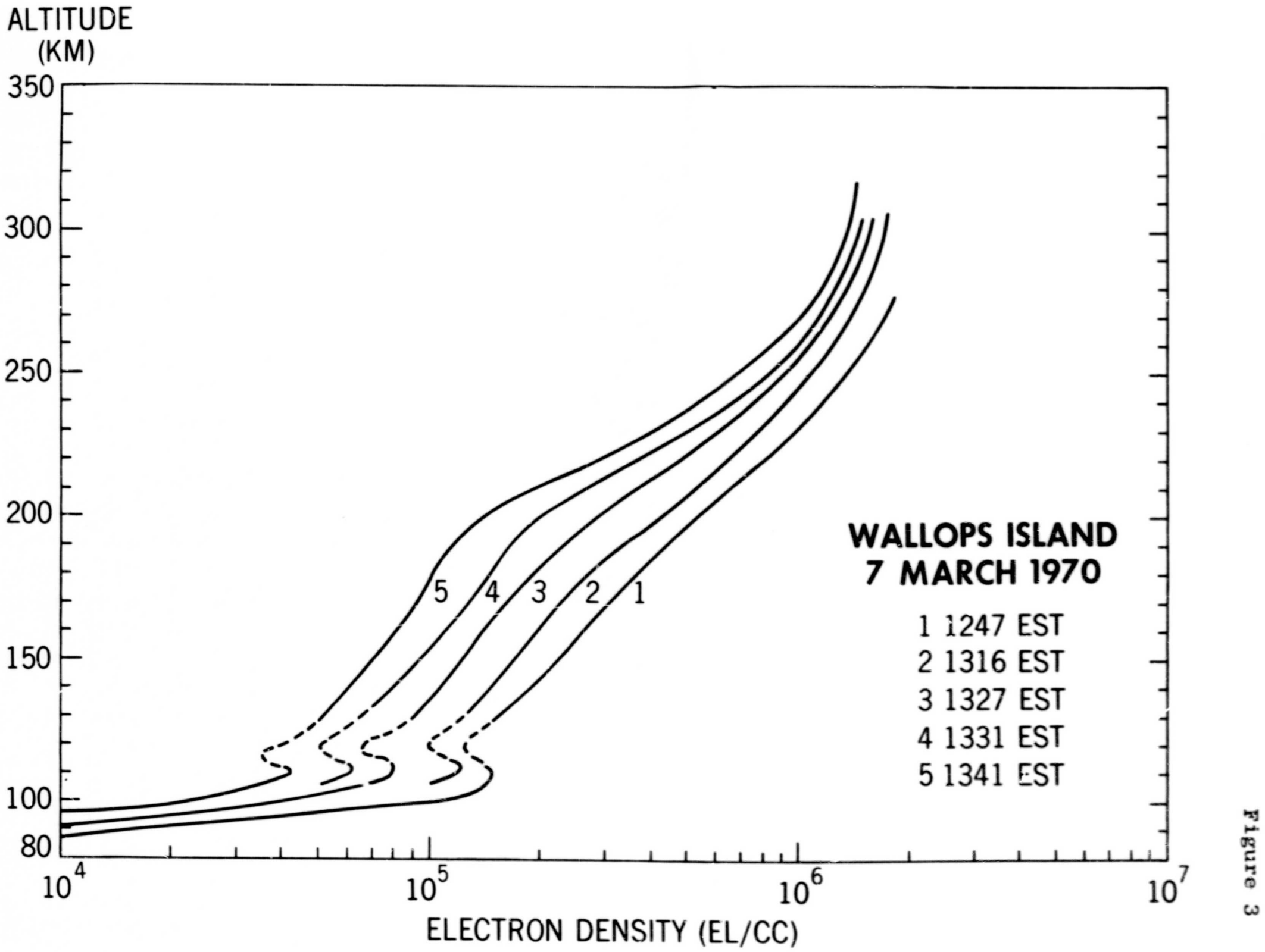
ALTITUDE
(KM)
350
300
250
200
150
100
80
5
4
3
2
1
WALLOPS ISLAND
7 MARCH 1970
1 1247 EST
2 1316 EST
3 1327 EST
4 1331 EST
5 1341 EST
10^4
10^5
10^6
10^7
ELECTRON DENSITY (EL/CC)

Figure 3

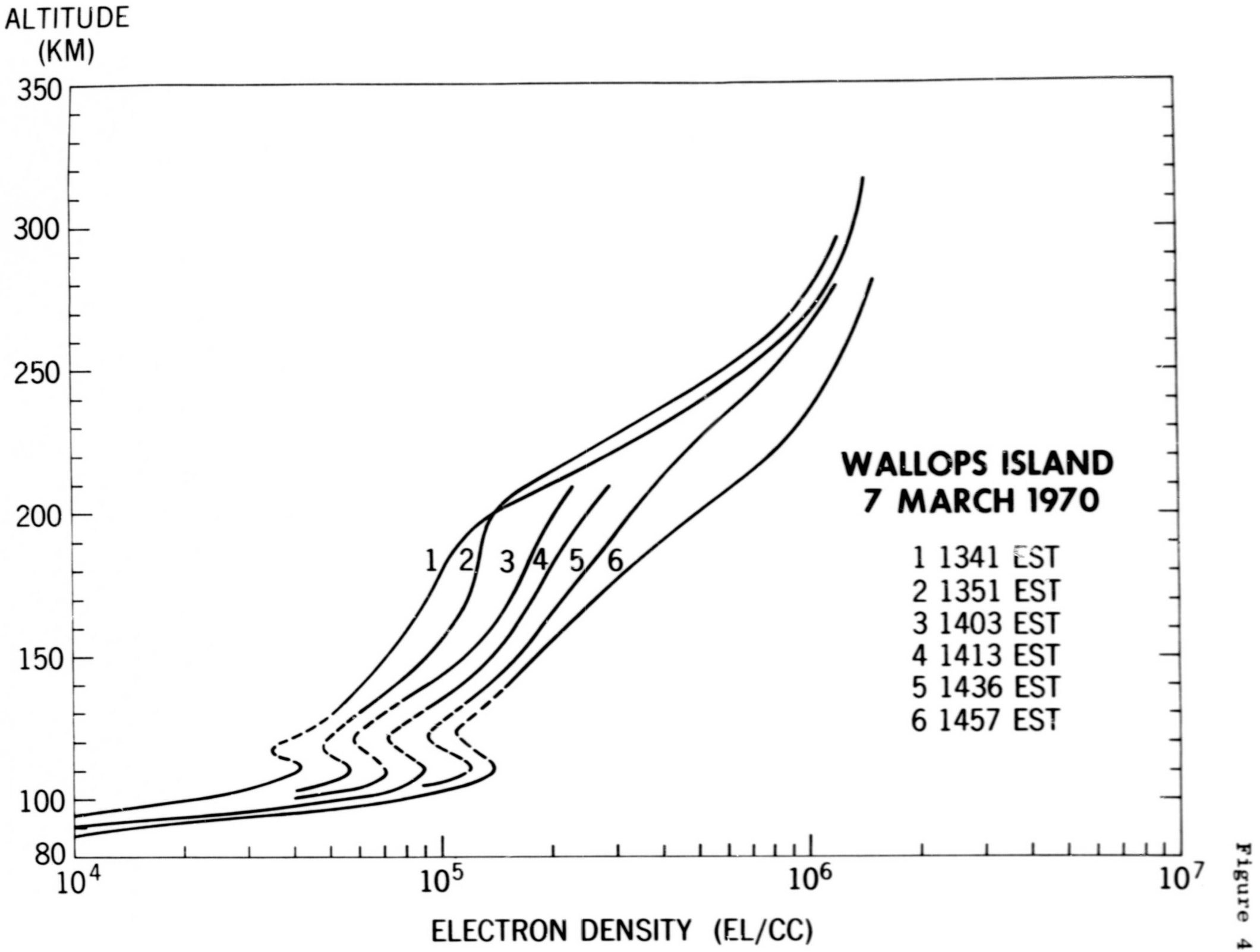
ALTITUDE
(KM)
350
300
250
200
150
100
80
10^4
10^5
10^6
10^7
ELECTRON DENSITY (EL/CC)
1
2
3
4
5
6
WALLOPS ISLAND
7 MARCH 1970
1 1341 EST
2 1351 EST
3 1403 EST
4 1413 EST
5 1436 EST
6 1457 EST

Figure 4

Figure 5

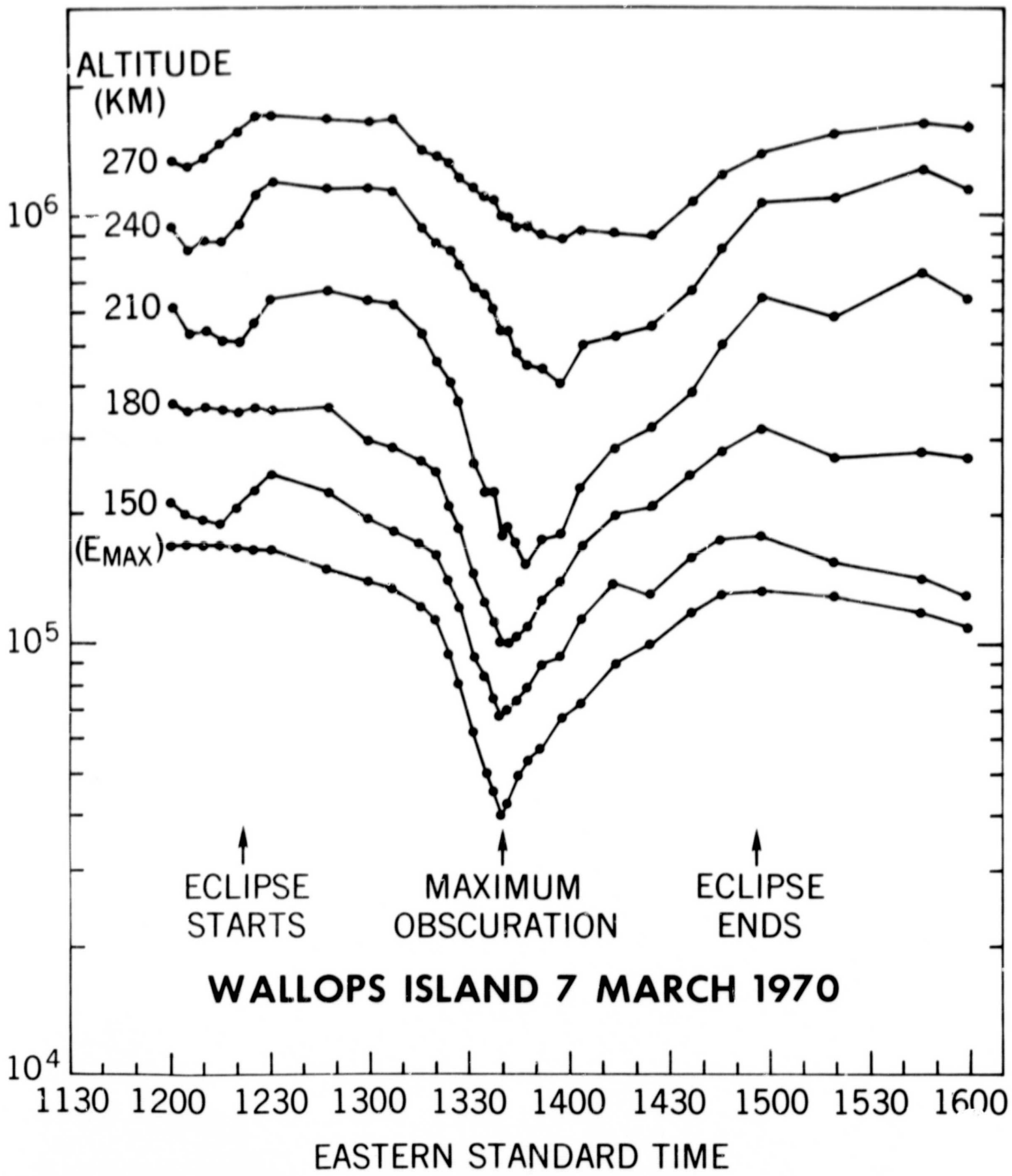
ALTITUDE
(KM)
270
240
210
180
150
(EMAX)
10^6
10^5
10^4
ECLIPSE
STARTS
MAXIMUM
OBSCURATION
ECLIPSE
ENDS
WALLOPS ISLAND 7 MARCH 1970
1130 1200 1230 1300 1330 1400 1430 1500 1530 1600
EASTERN STANDARD TIME

Figure 6

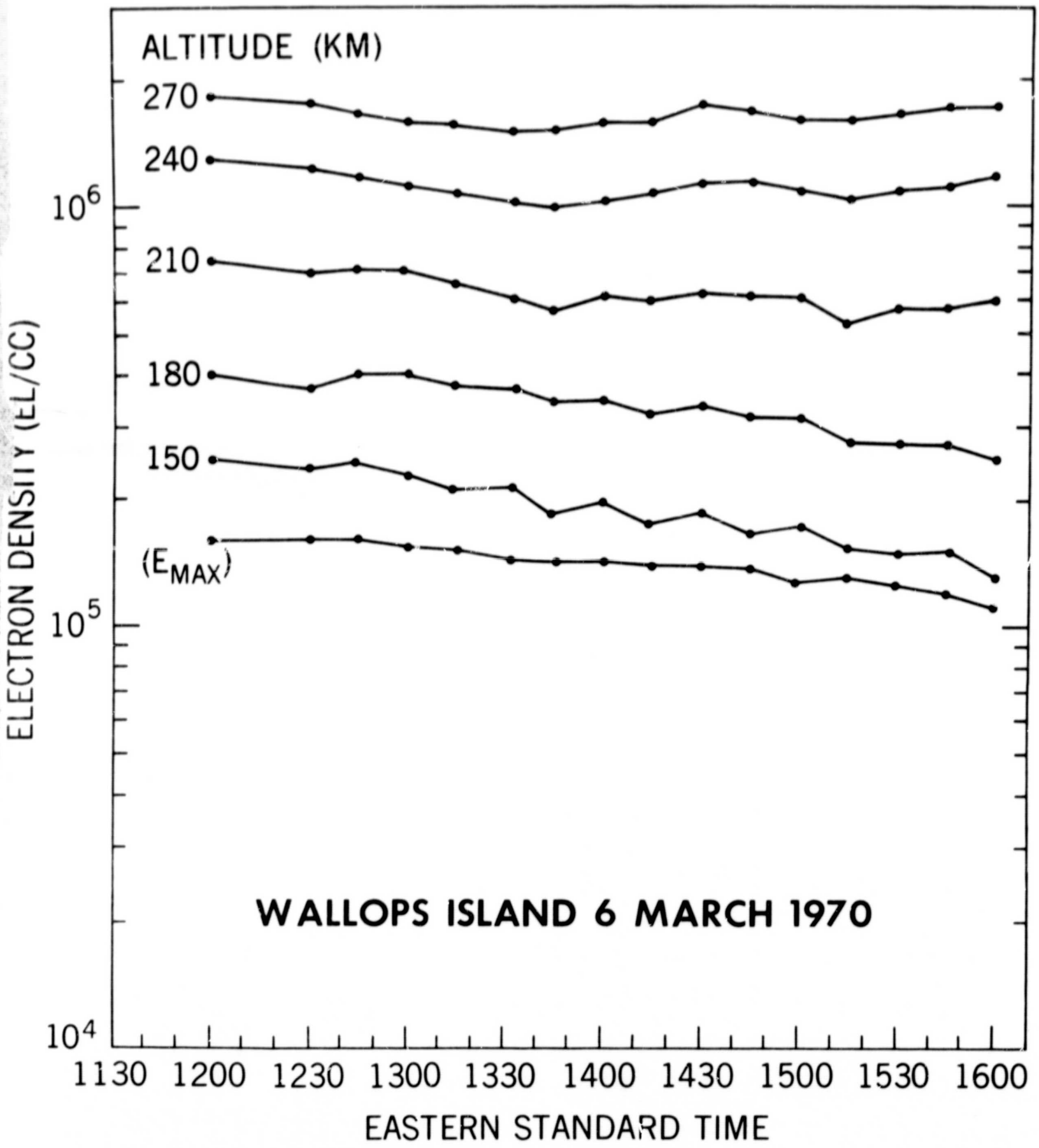
ALTITUDE (KM)
270
240
210
180
150
(E_MAX)
10^6
10^5
10^4
ELECTRON DENSITY (EL/CC)
WALLOPS ISLAND 6 MARCH 1970
1130 1200 1230 1300 1330 1400 1430 1500 1530 1600
EASTERN STANDARD TIME

Figure 7

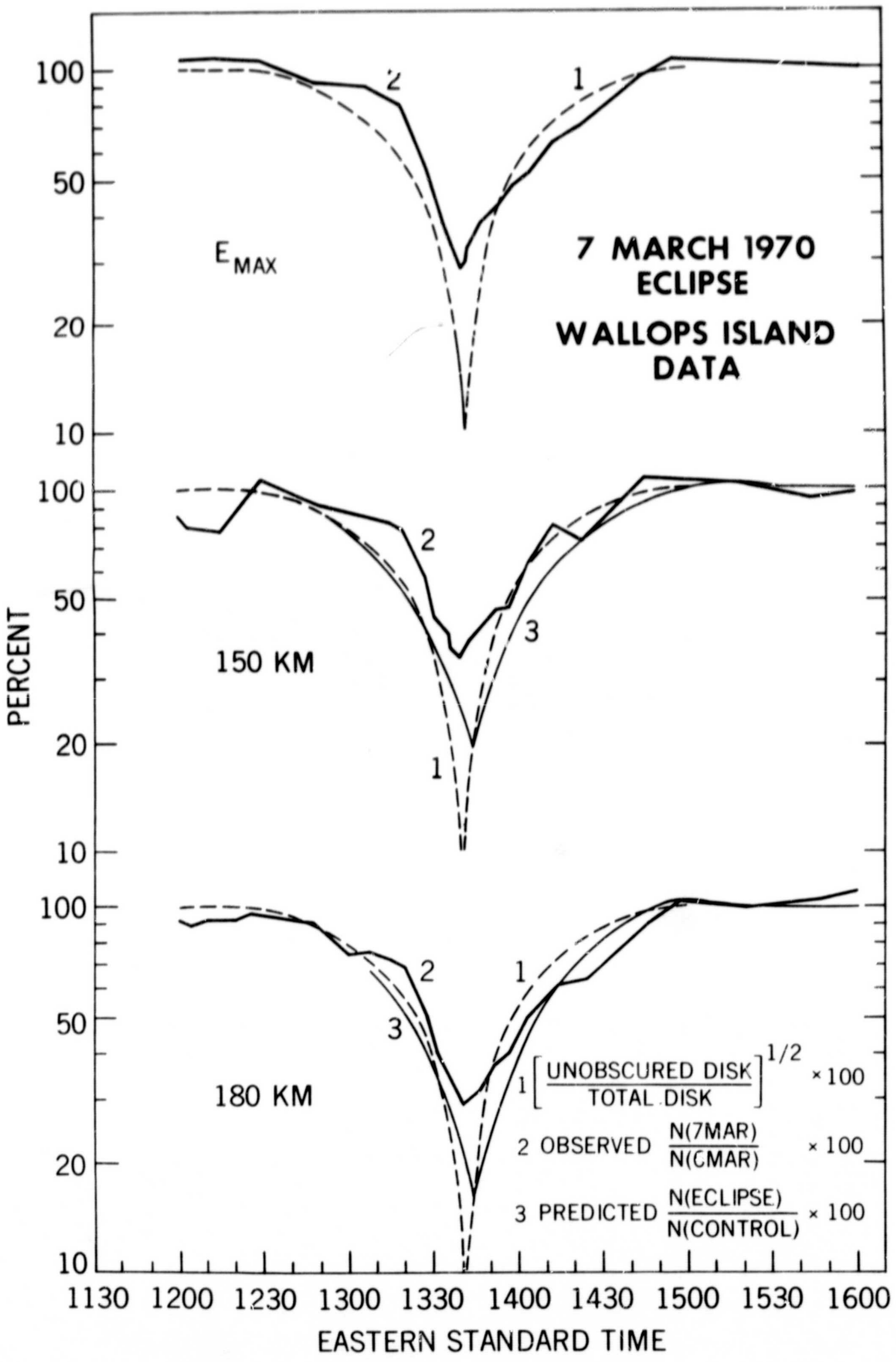
100
50
20
10
E_{MAX}
2
1
7 MARCH 1970
ECLIPSE
WALLOPS ISLAND
DATA
PERCENT
150 KM
180 KM
3
$1\left[\frac{\text{UNOBSCURED DISK}}{\text{TOTAL DISK}}\right]^{1/2} \times 100$
2 OBSERVED $\frac{N(7MAR)}{N(CMAR)} \times 100$
3 PREDICTED $\frac{N(ECLIPSE)}{N(CONTROL)} \times 100$
1130 1200 1230 1300 1330 1400 1430 1500 1530 1600
EASTERN STANDARD TIME

Figure 8

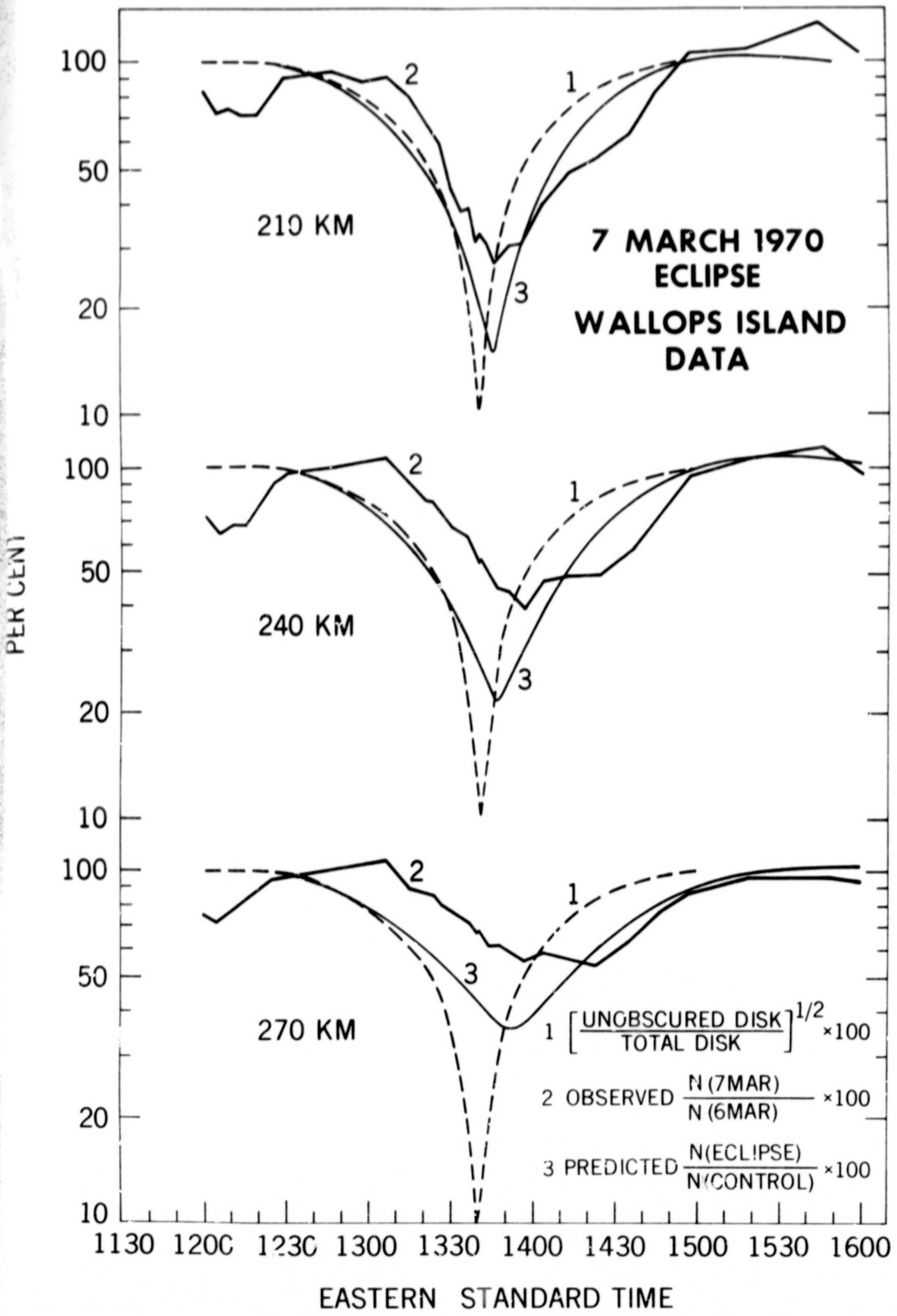

Figure 9

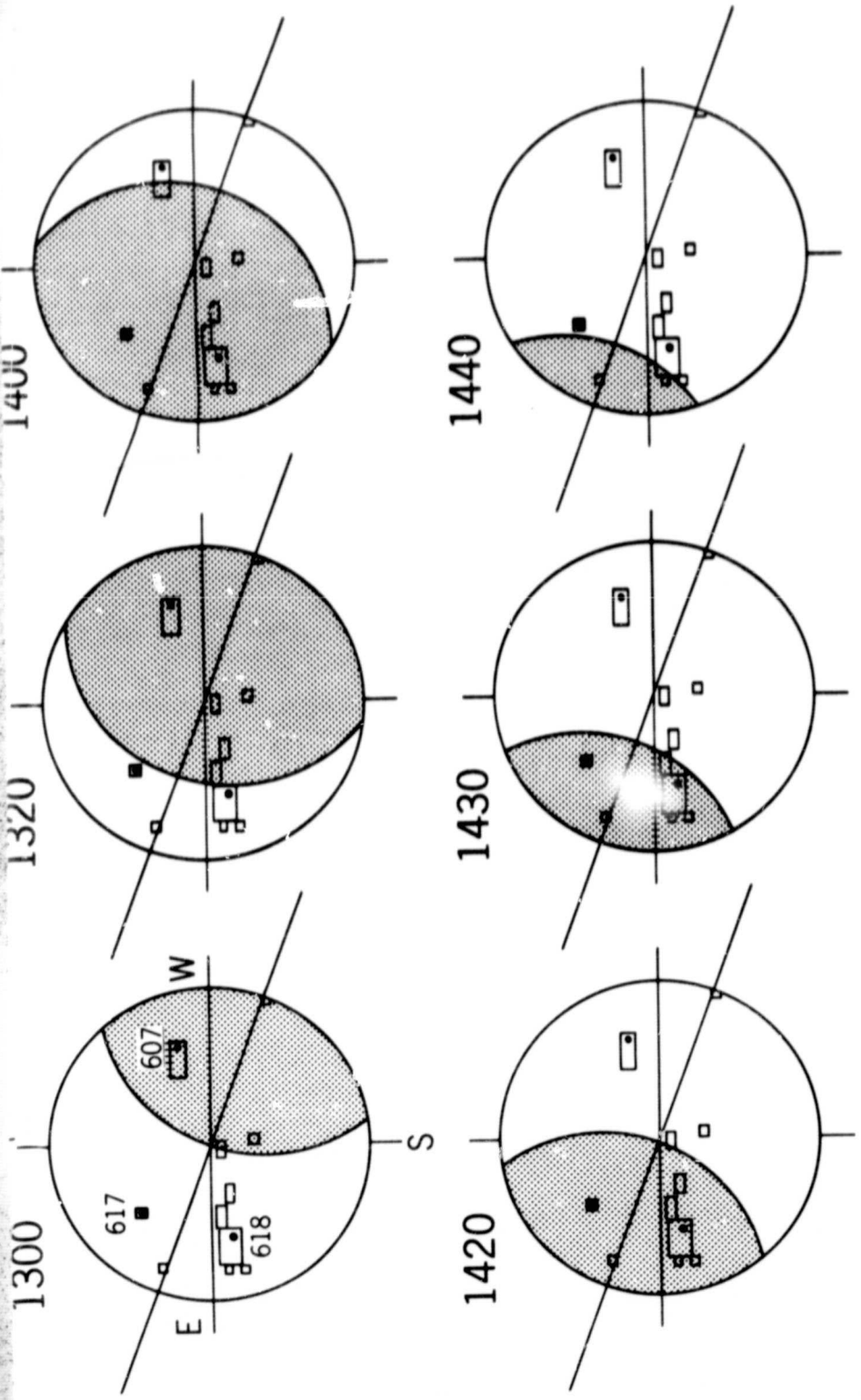

Figure 10

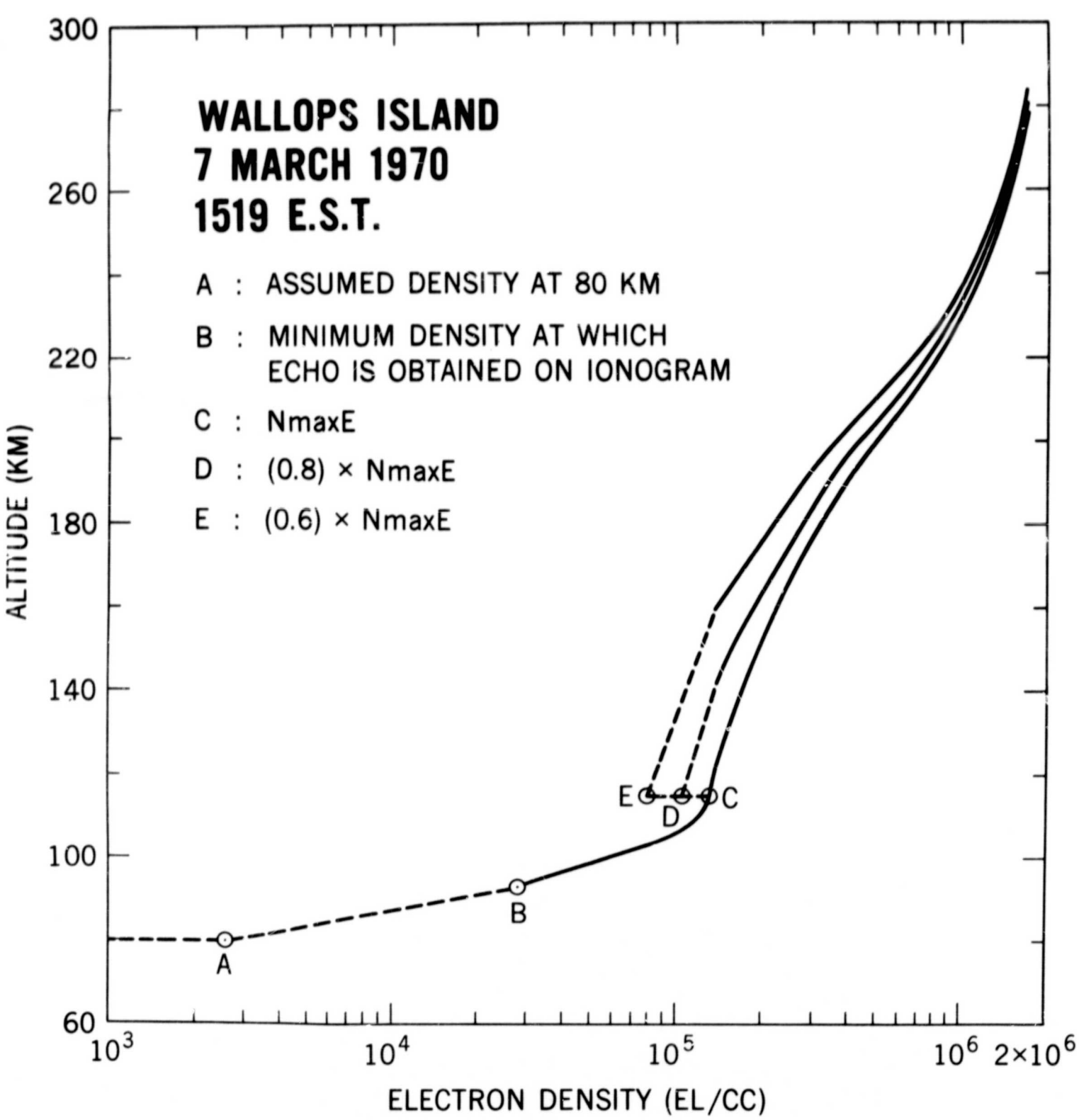
WALLOPS ISLAND
7 MARCH 1970
1519 E.S.T.
A : ASSUMED DENSITY AT 80 KM
B : MINIMUM DENSITY AT WHICH ECHO IS OBTAINED ON IONOGRAM
C : NmaxE
D : (0.8) × NmaxE
E : (0.6) × NmaxE
ALTITUDE (KM)
300
260
220
180
140
100
60
A
B
C
D
E
10^3
10^4
10^5
10^6
2×10^6
ELECTRON DENSITY (EL/CC)

Figure 11

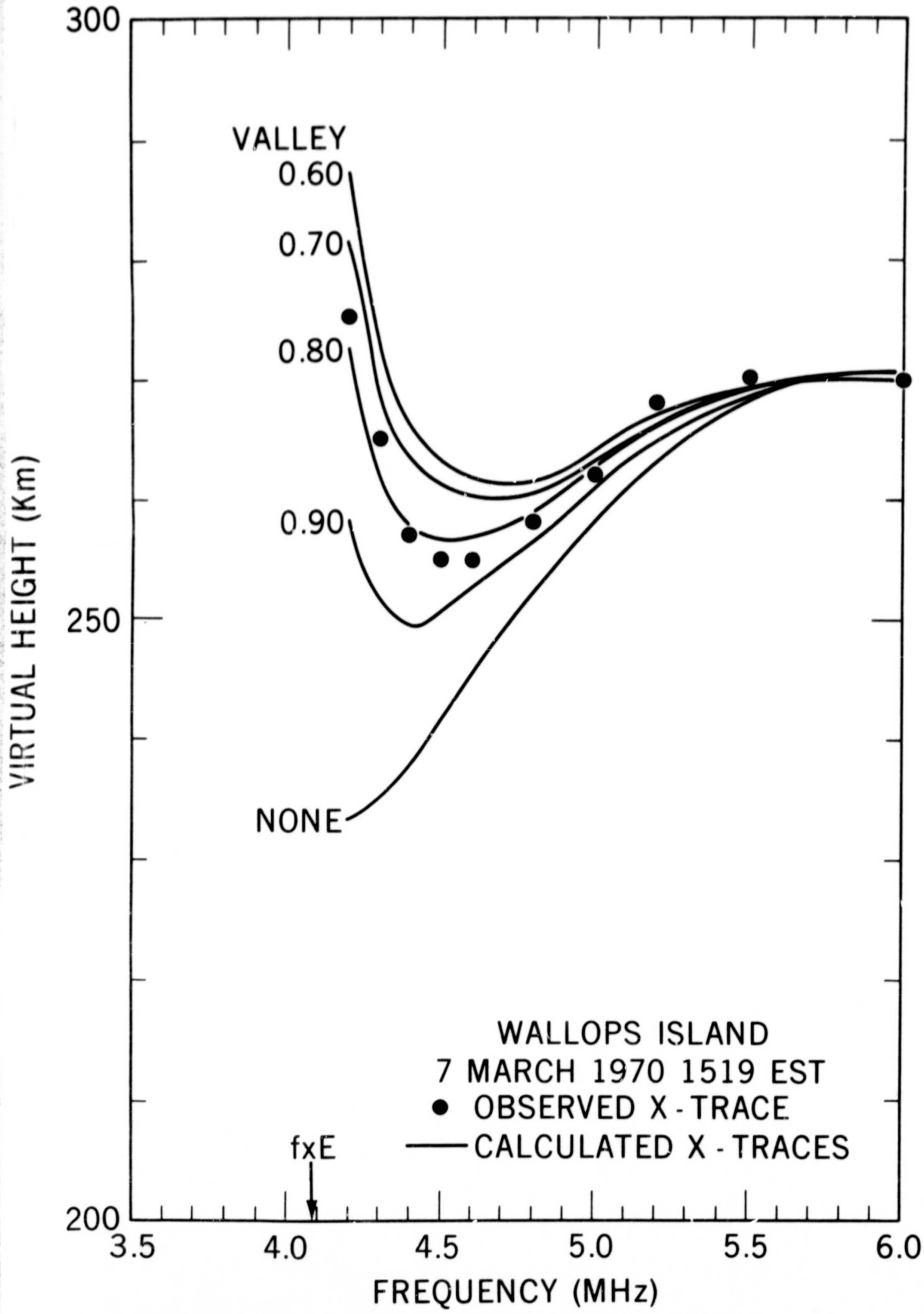
300
VALLEY
0.60
0.70
0.80
0.90
NONE
250
200
VIRTUAL HEIGHT (Km)
WALLOPS ISLAND
7 MARCH 1970 1519 EST
OBSERVED X-TRACE
CALCULATED X-TRACES
fxE
3.5
4.0
4.5
5.0
5.5
6.0
FREQUENCY (MHz)

Figure 12

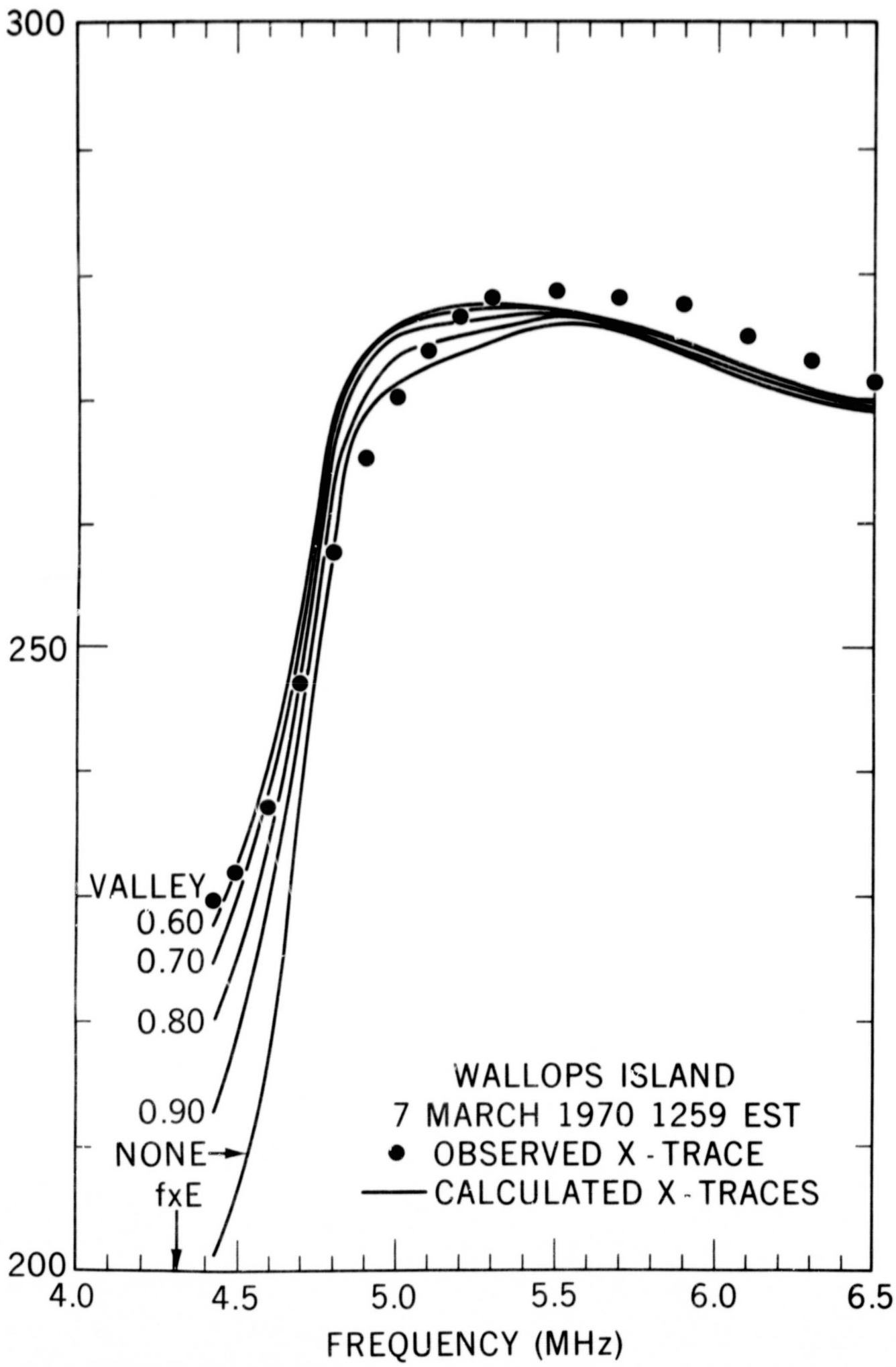
300
250
200
VIRTUAL HEIGHT (Km)
VALLEY
0.60
0.70
0.80
0.90
NONE
fxE
WALLOPS ISLAND
7 MARCH 1970 1259 EST
OBSERVED X-TRACE
CALCULATED X-TRACES
4.0
4.5
5.0
5.5
6.0
6.5
FREQUENCY (MHz)